Cumulative growth and stress responses to the 2018-2019 drought in a European floodplain forest

Florian Schnabel[1,2,*], *Sarah Purrucker*[2], *Lara Schmitt*[2], *Rolf A. Engelmann*[1,2], *Anja Kahl*[2], *Ronny Richter*[1,2,3], *Carolin Seele-Dilbat*[2,4], *Georgios Skiadaresis*[5], *Christian Wirth*[1,2,6]

*Corresponding author: florian.schnabel@idiv.de

Affiliations

[1]German Centre for Integrative Biodiversity Research (iDiv) Halle-Jena-Leipzig, Leipzig, Germany

[2]Systematic Botany and Functional Biodiversity, Leipzig University, Leipzig, Germany

[3]Geoinformatics and Remote Sensing, Leipzig University, Leipzig, Germany

[4]Department of Conservation Biology, Helmholtz Centre for Environmental Research (UFZ), Leipzig, Germany

[5]Chair of Silviculture, Institute of Forest Sciences, Freiburg University, Freiburg, Germany

[6]Max-Planck Institute for Biogeochemistry, Jena, Germany

ORCID IDs

F.S. (0000-0001-8452-4001); R.R. (0000-0002-8728-7918); G.S. (0000-0002-2385-0476); C.W. (0000-0003-2604-8056)

Abstract

Droughts increasingly threaten the world's forests and their potential to mitigate climate change. In 2018-2019, Central European forests were hit by two consecutive hotter drought years, an unprecedented phenomenon that is likely to occur more frequently with climate change. Here, we examine trees' growth resistance and physiological stress responses (increase in carbon isotope composition; $\Delta\delta^{13}C$) to this consecutive drought based on tree-rings of dominant tree species in a Central European floodplain forest. Tree growth was not reduced for most species in 2018, indicating that water supply in floodplain forests can partly buffer meteorological water deficits. Drought stress in 2018 was comparable to former single drought years, but the cumulative drought stress in 2019 induced drastic decreases in growth resistance and increases in $\Delta\delta^{13}C$ across all species. Consecutive hotter droughts pose a novel threat to forests under climate change, even in forest ecosystems with high levels of water supply.

Introduction

The frequency and intensity of droughts and corresponding surges of forest dieback events around the globe are projected to increase in the 21st century[1,2]. This critically endangers the world's forests and the variety of ecosystem services they sustain, such as their potential to act as carbon sink[3] and as a nature-based solution for climate change mitigation[4]. Recent drought events, moreover, belong to a new category, so called 'hotter droughts', where low precipitation coincides with heat waves, which creates a positive feedback loop between soil-water depletion through evapotranspiration and increased surface temperatures through reduced cooling by latent heat production[5,6]. In 2018-2019, Central Europe has been hit by two consecutive and hotter summer drought events, a phenomenon unprecedented at least in the last 250 years but likely to occur more

46 frequently with intensifying climate change[7]. The 2018 hotter drought alone had already stronger
47 negative effects on European ecosystems than the formerly severest drought event in 2003[5] and
48 induced widespread premature leaf senescence and tree mortality[8]. An increasing number of
49 studies has shown that droughts can affect tree growth and hence carbon cycling in forests for
50 years after the actual drought event and that such 'legacy effects' are widespread in forest
51 ecosystems[9–13]. The consecutive hotter drought in 2019 may thus have critically amplified drought
52 stress as trees were hit that already had emptied carbon reserves, impaired hydraulic functioning
53 due to embolism and weakened defense systems[8,13] and only access to emptied soil water reserves.
54
55 Drought effects on forests can be analyzed retrospectively through analyses of tree-rings, which
56 are an archive of past growing conditions including climate and water availability[14]. In
57 dendroecology the annual growth of trees (i.e. the width of tree rings formed each year) is a
58 principle indicator of drought effects, which can be analyzed through quantifying growth
59 resistance to drought (hereafter 'growth resistance')[15,16]. Growth resistance quantifies the ability
60 of a tree to withstand drought stress through comparing growth in drought years with mean growth
61 in a reference period, i.e. years with 'normal' climate conditions prior to the drought event[15]. Such
62 growth resistance analyses may be especially suitable when rapid impact assessments are needed
63 and no data is available on the post disturbance period. Next to growth, the carbon isotope ratio of
64 ^{13}C to ^{12}C in wood – called $\delta^{13}C$ – is a widespread physiological indicator of a tree`s water status
65 and drought stress[17–19]. The $\delta^{13}C$ composition in tissues of C_3 plants like most trees is a record of
66 the ratio between intercellular and ambient CO_2 concentration during the time of carbon fixation
67 that is modulated by both, CO_2 assimilation and stomatal aperture[19]. Under ample water supply
68 and fully open stomata, plants discriminate against the heavier ^{13}C in favor of the lighter ^{12}C.

69 However, under water shortage, stomatal conductance is stronger down-regulated than
70 assimilation, which induces an increase of $\delta^{13}C$ in the wood formed during drought[17,19]. Thus,
71 drought stress can be quantified as increase in wood carbon isotope ratio ($\Delta\delta^{13}C$) between drought
72 and normal years. Hence, growth resistance and $\Delta\delta^{13}C$ combined provide a powerful tool to
73 quantify drought effects on trees.
74
75 Tree species vary greatly in their susceptibility to drought due to physiological and morphological
76 differences. Among other features such as cavitation resistance[20] two key factors that might drive
77 tree species reactions to drought are stomatal control and root system architecture[21–23]. Stomatal
78 closure in response to water deficits enables plants to avoid critically low water potentials through
79 transpiration losses and thus hydraulic failure but species differ largely in their type of stomatal
80 control[21,22]. Isohydric or water saving species close their stomata fast during water shortage, while
81 anisohydric or water spending species keep their stomata open and continue to transpire.
82 Consequently, the latter strategy necessitates continued water uptake via roots and carries an
83 increased risk for xylem cavitation[21]. While isohydric species may thus show earlier growth and
84 $\Delta\delta^{13}C$ responses, anisohydric species may face high cavitation risks during severe and prolonged
85 drought conditions characterized by very low soil moisture availability. Next to stomatal control,
86 root system architecture varies strongly between species[23–25] and may influence drought responses
87 as shallow-rooting species likely lose access to soil water faster than deep-rooting species that can
88 access the deeper and still moist layers[26]. Hence, for understanding and generalizing the effects of
89 consecutive droughts on forests, tree species should be examined that span a gradient in such traits.
90

The high tree species richness of floodplain forests[27] makes them ideally suited for comparative studies of tree species reactions to consecutive droughts as they are one of the few systems where coexisting mature trees spanning an entire gradient of hydraulic behaviors can be found. Floodplain forests rank among the most rapidly disappearing ecosystems due to land conversion and drainage[23,28] and novel climatic conditions – like prolonged droughts – may amplify this trend through changing the hydrological regimes on which these forests depend. For instance, sinking groundwater levels may increase tree growth sensitivity to drought and susceptibility to drought-induced dieback[23,29] and this might bring these forests, which are among the most dynamic, productive and diverse Central European habitats[30,31], closer to a tipping point. On the contrary, the higher water availability in floodplain forests may buffer drought effects to a certain extent as trees might have access to groundwater in addition to precipitation-derived moisture[32]. Hence, it is conceivable that if drought effects on resistance and $\Delta\delta^{13}C$ were observed in floodplain trees, other forest ecosystems might experience even stronger effects.

Here, we focus on the effect of the two consecutive drought years 2018-2019 characterized by extremely hot and dry conditions (Fig. 1), as well as their cumulative effects, on tree growth resistance and $\Delta\delta^{13}C$ as physiological stress response. To this end, we reconstruct the stress exerted by this unprecedented event and compare it to past (single) drought events based on tree-ring records from dominant tree species in the Leipzig floodplain forest, one of the few remaining and thus highly protected floodplain forests in Central Europe[33,34]. The studied species span a gradient in stomatal control and root system architecture, with *Quercus robur* L. (hereafter oak) having isohydric behavior[35,36] and a deep reaching heart-sinker root system[24,25], *Acer pseudoplatanus* L. (hereafter maple) having an intermediate (rather isohydric) stomatal control[37,38] and rooting

114 depth[25] and *Fraxinus excelsior* L. (hereafter ash) having an anisohydric behaviour[37,38] and an
115 allocation of most roots to shallow soil layers[24,25]. This gradient allowed us to explore a broad
116 range of species response strategies to consecutive drought stress. We sampled trees in two
117 environmental strata representing topographic differences in distance to groundwater. We expect
118 the results for the hypotheses proposed below to be more pronounced in the dryer stratum.
119 Specifically, we tested the following hypothesis:
120
121 **H1** Drought stress in 2018 – measured as decreased growth resistance and a positive $\Delta\delta^{13}C$ – is
122 comparable to the stress experienced during former drought years. High groundwater levels in
123 floodplain forests buffer effects of such single drought years.
124
125 **H2** The consecutive drought years 2018-2019 lead to a drastically decreased growth resistance and
126 a further increase in $\Delta\delta^{13}C$ in 2019.
127
128 **H3** Isohydric species respond faster to drought stress (already in 2018), while anisohydric species
129 react later but show stronger reactions to the consecutive drought in 2019.
130

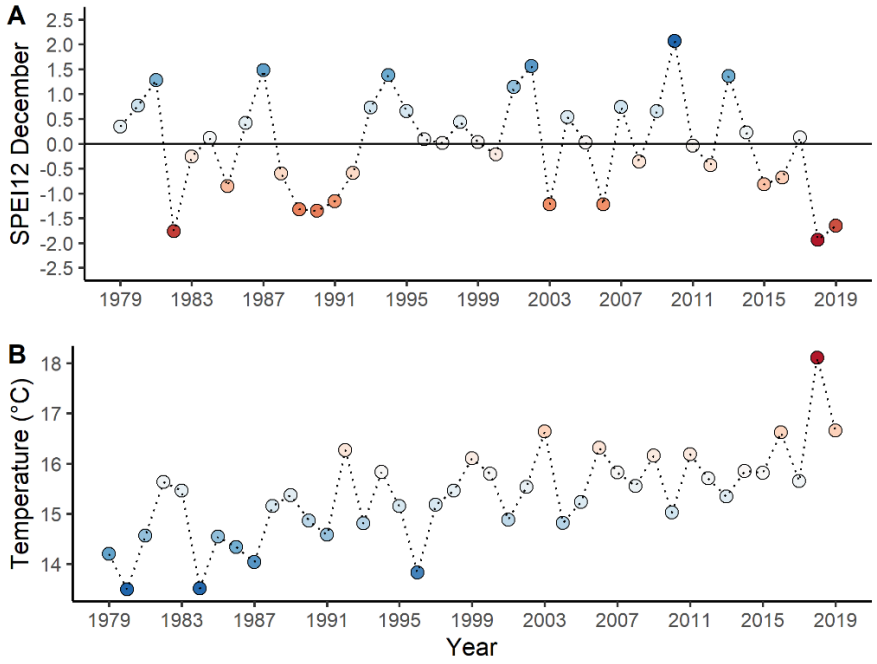

Fig. 1 Annual standardized water balance of precipitation minus potential evapotranspiration (A, January-December) and mean growing season temperature (B, April-September) per year from 1979-2019 in the Leipzig floodplain forest. The water balance was calculated as Standardized Precipitation Evapotranspiration Index (SPEI[39]). Points are colored according to their value with deeper red indicating increasing drought and heat wave severity. The horizontal line in (A) represents the long-term mean, negative values indicate water deficits and positive values water surpluses. SPEI values below -1 and above 1 can be considered exceptionally dry and wet, respectively. See Supplementary Figs. 1-2 for additional SPEI lengths, climatic and hydrological variables that we used to identify drought events.

Results

We found pronounced responses to drought stress in terms of tree growth and $\Delta\delta^{13}C$ across the examined tree species, with strongest stress responses in the second of two consecutive drought years (2019). Mean growth resistance in single drought years before the 2018-2019 consecutive

145 drought (hereafter 'single drought years') ranged around zero for oak and maple, while growth
146 resistance in ash tended to be below zero (Fig. 2a-c). This indicates a similar tree growth in single
147 drought years and in climatically 'normal' years for oak and maple but not for ash (drought year
148 classification based on the Standardized Precipitation Evapotranspiration Index (SPEI)[39]; see
149 methods). Growth of oak and maple even tended to be higher in 2018 compared to normal years
150 (mean growth resistance above zero). The hotter drought in 2018 did not induce significant
151 reductions in growth resistance in oak and maple compared to single drought years ($P>0.1$ for both
152 species) but growth resistance in ash decreased significantly ($t=-2.94$, $P=0.004$; Fig. 2c;
153 Supplementary Table 1). In 2019, the second consecutive and extreme drought year, growth
154 resistance of all species dropped drastically in comparison to single drought years (oak $t=-2.00$,
155 $P=0.049$; maple $t=-2.74$, $P=0.008$; ash $t=-7.22$, $P<0.001$; Fig. 2a-c; Supplementary Table 1) and in
156 comparison to 2018 (Supplementary Table 2). The trends in growth resistance were insensitive to
157 the type of growth data (raw or detrended) and reference period (1-year or pooled years) used
158 (Supplementary Figs. 3-4). Distance to groundwater had an overall small influence on the growth
159 resistance of the examined species (non-significant interaction of drought year and groundwater
160 level). Only for oak we found indications for a higher growth resistance on wet plots in 2019
161 (significant interaction of drought year and groundwater level, $P=0.0413$). Among the three
162 analysed species, ash showed the highest growth sensitivity to drought (especially to SPEIs
163 indicating summer drought) while oak was the least sensitive (Supplementary Fig. 5).
164

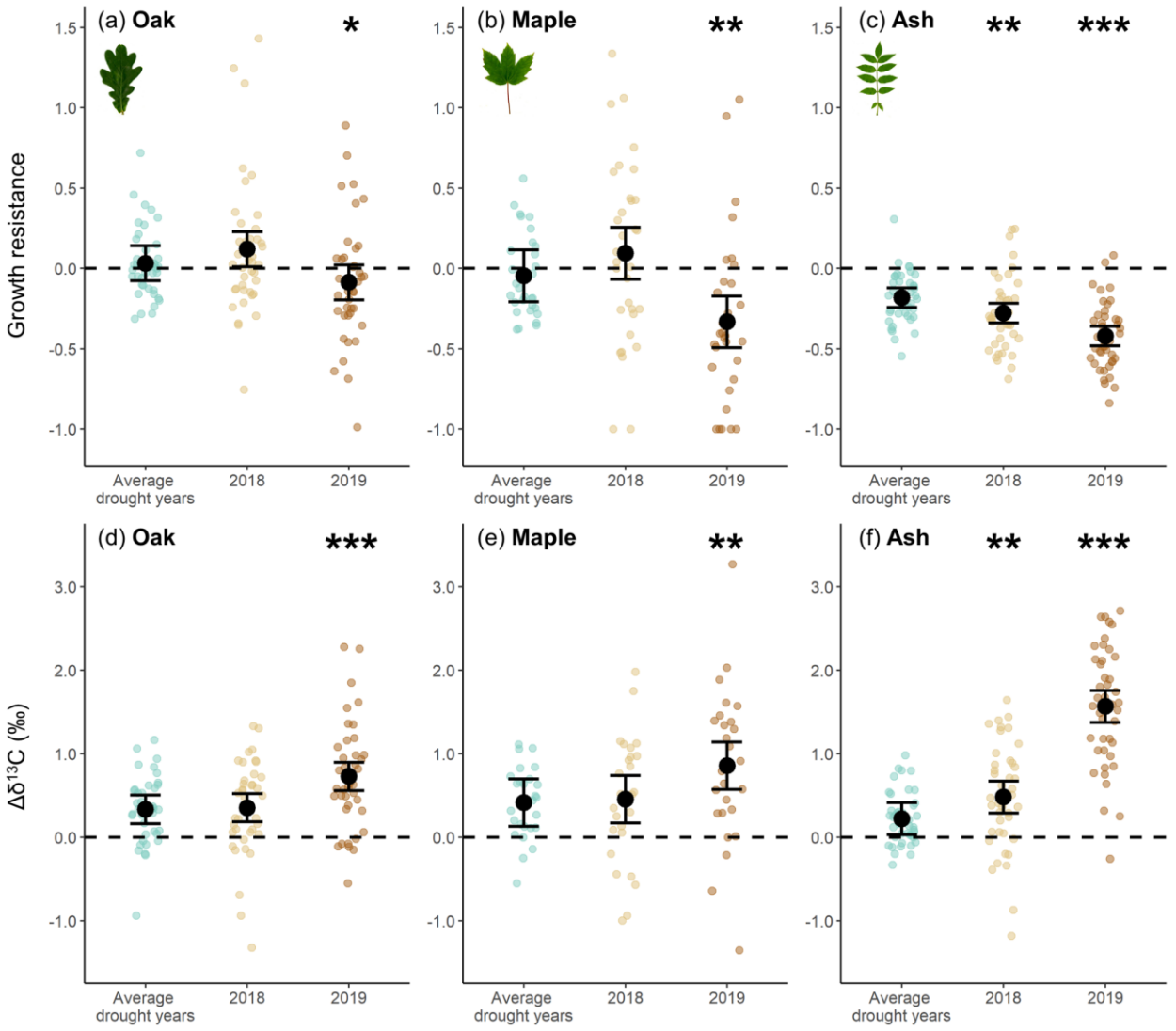

Fig. 2 Growth resistance and increase in the carbon isotope ratio ($\Delta\delta^{13}C$) in wood of oak, maple and ash in drought years. The figure shows growth resistance (upper panels) and $\Delta\delta^{13}C$ (lower panels) in the consecutive hotter drought years 2018 and 2019 compared to the mean resistance and $\Delta\delta^{13}C$ in single drought years (2003, 2006 and 2015). A value around 0 corresponds to a comparable growth and $\delta^{13}C$ in drought and normal years. Black points show estimated marginal means and error bars the 95% confidence intervals of linear mixed-effect model fits. Coloured points show growth resistance and $\Delta\delta^{13}C$ values per tree and species (oak n=40, n=39; maple n=32, n=26; ash n=42, n=42) and are jittered to enhance visibility. Growth resistance and $\Delta\delta^{13}C$ were calculated with Eq. 1 and Eq. 3, respectively. The tree ring-widths have been detrended with a negative exponential function. Statistically significant differences in growth

resistance and $\Delta\delta^{13}C$ between the years 2018 and 2019 compared to single drought years are indicated by asterisks over the respective year ('***' p <0.001; '**' p <0.01; '* 'p <0.05).

We found positive $\Delta\delta^{13}C$ values across all species and drought years, indicating tree physiological stress responses to drought irrespective of drought type (single or consecutive; Fig. 2d-f). However, the magnitude of $\Delta\delta^{13}C$ increases varied strongly between drought years and species. For oak and maple, $\Delta\delta^{13}C$ was not significantly enhanced in 2018 compared to single drought years (P=0.85 and P=0.79), while ash had significantly lower $\Delta\delta^{13}C$ values (t=2.85, P=0.006; Fig. 2f; Supplementary Table 1). Across all species, we found a drastic increase in $\Delta\delta^{13}C$ in 2019 compared to single drought years (oak t=3.93, P<0.001; maple t=2.80, P=0.007; ash t=14.80, P<0.001; Fig. 2d-f; Supplementary Table 1) and in comparison to 2018 (Supplementary Table 2). The $\Delta\delta^{13}C$ increase was strongest for ash. Distance to groundwater had no significant influence on $\Delta\delta^{13}C$ for all examined species. Together these results indicate that drought stress in 2018 was, except for ash, comparable to stress in former single drought years, while the second consecutive drought year 2019 induced unprecedented growth reductions and increases in $\Delta\delta^{13}C$ across all species.

Discussion

Using tree growth resistance and $\Delta\delta^{13}C$ as indicators of drought stress, we report a drastic increase in drought-related stress in the second of two consecutive hotter drought years across all examined species. Drought responses were strikingly consistent for both indicators (growth resistance and $\Delta\delta^{13}C$; Fig. 2), but the timing and magnitude of responses were species-specific: Oak showed the overall smallest stress response followed closely by maple with the strongest response in ash. The

198 2019 drought, although an extreme drought as well, was meteorologically less severe than the
199 preceding drought year 2018, as indicated by less negative SPEI values and lower growing season
200 temperature (Fig. 1). This indicates that the cumulative drought effect exerted by both years was
201 responsible for the stress increase in 2019. The 2018 hotter drought was the severest drought so
202 far recorded in Central Europe[5,7,8], but, as predicted, we found drought stress to be comparable to
203 former single drought years and tree growth to be largely within the range of climatically 'normal'
204 years. Hence, the high water availability in floodplain forests may partly buffer tree stress
205 responses to single but not to consecutive drought years.
206
207 Our conclusion that the effects of single drought years were buffered to some extent contrasts with
208 the dramatic drought effects reported across European forests in 2018 that suffered widespread
209 defoliation, xylem hydraulic failure and mortality[5,8] but is consistent with other floodplain forest
210 studies. For instance, the exceptionally high gross primary production during the warm spring in
211 2018 was found to compensate for losses later that year due to drought in a Czech floodplain
212 forest[31]. Similarly, tree growth recovered within two years after the 1976 drought for all herein
213 analyzed floodplain forest species, which was attributed to the drought buffering effect of water
214 availability in floodplain forests[32]. Nonetheless, we found physiological stress increases ($\Delta\delta^{13}C$)
215 in 2018 while tree growth in most species did not react. This confirms the view of more consistent
216 drought signals in $\Delta\delta^{13}C$ compared to tree ring-width[18], potentially due to tree growth being
217 maintained from carbon reserves even under low soil water availability[18].
218
219 This picture changed dramatically in 2019. As hypothesized, we observed drastic stress increases
220 in the second consecutive drought year, likely driven by the cumulative effect of both drought

years. Drought legacy effects[9] were found to be widespread in forests and to effect tree growth and $\Delta\delta^{13}C$ 1-5 years after the actual drought event[9–13,15]. Hence, trees were likely still suffering from 2018 when the second drought year 2019 stroke. Results on drought legacies from former studies are, however, only partially applicable to our case, as these focused on legacy effects in post drought periods in which trees where already (partially) recovering. In such cases it is difficult to disentangle drought legacy effects from other changes in a trees environment that may affect tree growth and $\Delta\delta^{13}C$[12]. In contrast, we focus here on two consecutive hotter drought years, unprecedented in their severity at least since 250 years[7], which left the trees no time to recover. The few studies that studied prolonged droughts, moreover, did not examine the cumulative built-up of drought effects from year-to-year as they used either mean tree growth across drought years or growth in the last year of drought to calculate growth resistance[16]. In comparison, the strong reactions we report for 2019 should be clearly attributable to legacies of 2018, as other changes in the trees' environment like reduced competition for light are unlikely within a single year. In addition, forest management can be excluded as potential cause as we did not sample trees in stands that experienced recent interventions. Similarly, assessments of the 2018 hotter drought found early signs of strong drought legacy effects[5,8].

Different meteorological conditions may have amplified this cumulative drought stress. The increasing frequency of droughts and exceptionally hot years, especially since 2015[8] (Fig. 1; Supplementary Fig. 1), may have successively reduced the trees capacity to withstand drought[13], leaving them weakened when the 2018-2019 drought stroke[5]. Moreover, the second hotter drought year 2019 started already with severe water shortages as the low winter and spring precipitation in 2018-2019 was not enough to refill soil water reservoirs (UFZ Drought Monitor/Helmholtz Centre

for Environmental Research). Finally, the severe drought conditions in both years coincided with the main growth period of the trees (April-August)[5,40] and thus exerted the highest possible stress. Our sampling sites cover the whole gradient of groundwater conditions in the examined floodplain forest but interestingly we found only small effects of groundwater level. The reasons remain speculative. Differences in distances to the groundwater level may have been too small to induce strong effects on tree performance or, alternatively, more intense rooting on dry plots may have compensated for lower water availability[29]. It is also possible that trees depended primarily on water uptake from upper soil horizons that are fed through capillary rise from the groundwater level[24,41] which is broken under severe water shortage at all distances to the groundwater level.

Several physiological mechanisms could explain cumulative drought stress[9]. Drought-induced loss of leaves and xylem cavitation may impair growth and transpiration (and thus effect $\Delta\delta^{13}C$)[8,21]. Under consecutive drought, this damage persists, while vulnerability to cavitation may continue to increase under successive drought stress[13]. In the second drought year, less nonstructural carbohydrates (NSC) reserves were likely left for xylem repair, growth and especially for keeping up the trees defense system, which increases the susceptibility to pests and pathogens[8,13,21,42]. Large parts of the here examined stands suffered severe damages and mortality through sooty bark disease, ash dieback and secondary beetle infestations in 2019, which points to depleted NSC stores causing a collapse of the trees' immune system. We studied only the most vital tree individuals of the population thus largely excluding disease effects from our sample. However, as the majority of ash trees in the forest were affected to some degree[43], we cannot completely disentangle whether the species intrinsic traits, incipient ash-dieback or their interaction caused the strong stress response in this species. Finally, drought induces shifts in carbon allocation in

267 favor of the canopy and root system at the expense of radial growth[11] and, when photosynthesis is
268 insufficient to meet demands, NSC reserves are utilized to maintain autotrophic respiration, growth
269 and tissue repair[42,44]. This enriches the reserve pool and tissues built from it in ^{13}C as the
270 isotopically lighter ^{12}C is turned over faster than ^{13}C. Both processes may have further contributed
271 to the drastic decrease in tree-ring growth and increase in $\Delta\delta^{13}C$ in 2019 in addition to fractionation
272 through stomata closure.
273
274 The magnitude and timing of drought stress responses were species-specific, which may be related
275 to differences in species hydraulic traits. Oak has a deep reaching root system and may thus be
276 able to maintain water uptake during low precipitation periods[24,29,45], while its water saving
277 behavior (oak is isohydric[35,36]) may have helped to avoid xylem cavitation during peak drought
278 periods[21]. In contrast, ash has roots mainly restricted to upper soil layers and is thus more
279 dependent on precipitation than oak[23,24]. Its water spending behavior (ash is anisohydric[37,38]),
280 moreover, carries a high risk for xylem cavitation if continued water uptake via roots is impaired[21],
281 an especially risky strategy on the loamy Vega soils of our study site, which reached soil moisture
282 levels below the permanent wilting point of vegetation for clay soils[46] during the 2018 drought.
283 The intermediate stress reaction of maple is consistent with its stomatal control, which lies between
284 oak and ash[37,38]. This partly confirms our third hypothesis in that anisohydric ash showed the
285 strongest reaction to consecutive drought, but we did not find faster reactions to drought in 2018
286 in isohydric species (oak and maple). The intermediate drought reaction of maple, which is often
287 considered drought sensitive[37], may also be related to its less exposed crown position (maple trees
288 were rather co-dominant) which can reduce irradiance and water pressure deficits[47]. Finally, here
289 reported drought effects may be influenced through the naturally high tree species richness of

floodplain forests[27], as diverse tree communities may outperform species poor communities through complementarity in water use such as water uptake from different soil layers[24,48].

The response of forests to the increasing frequency and intensity of droughts[1] will affect a variety of ecosystem services and will determine if forests act as carbon sink or source in the 21st century. Here, we show that the cumulative effect of two consecutive hotter drought years (2018-2019) induces drastic drought-related tree stress responses in a Central European floodplain forest. We found partly buffered tree stress responses, presumably because floodplain trees are fed by groundwater in addition to precipitation, and examined only the most vital tree individuals of the population. Our results thus show a 'best-case scenario' and more severe tree responses could be expected if entire tree populations or other forest ecosystems were examined, as indicated by wide-spread tree mortality observed in assessments of the 2018 drought[5,8] and at our own site. Linking responses in growth resistance and $\Delta\delta^{13}C$ to tree mortality and carbon ecosystem fluxes remains challenging[11]. Moreover, it remains unknown how the here observed responses will affect tree recovery after and resilience[15,16] to (future) droughts. The strong drought legacy effects we observe in the second drought year (2019), the reported persistence of legacy effects for years[9] and successive declines in drought resistance under consecutive drought[13,15] are worrisome. On the other hand, a species like oak that combines a high tolerance to drought and flood[45], may remain resilient, underlining its importance for floodplain forests. Consecutive hotter droughts are projected to become more frequent[7]. Our ability to forecast forest responses to climate change hinges on our ability to understand what drives tree responses to this novel stress.

Methods

Study site

In this study, we used data collected from a Central European floodplain forest ecosystem located in the northwest of the city of Leipzig, Germany. The Leipzig floodplain forest is one of the few remaining and thus highly protected floodplain forests in Central Europe[33,34] and lies in the transition zone between maritime and continental climate characterized by warm summers, with an annual mean temperature of 9.6 °C and an annual precipitation sum of 525 mm (1979-2019; DWD, Station Leipzig/Halle). Its main rivers Weiße Elster, Luppe, Pleiße and Parthe formed the floodplain landscape, but their course and thus the floodplain forest itself has been strongly influenced by human interventions over the last centuries[49]. The straightening of rivers as well as dike and canal constructions strongly influenced the hydrological regime of the floodplain forest, which today does not experience regular flooding's anymore[50]. The contemporary floodplain forest ecosystem can be characterized as *Ficario-Ulmetum* Knapp ex Medwecka-Kornas 1952 (synonyms: *Fraxino-Ulmetum* Tüxen ex Oberdorfer 1953, *Querco-Ulmetum* Issler 1926 nom. inval.) with oak, elm and ash being the dominant tree species[51]. The absence of flooding, however, resulted in an on-going gradual shift to an oak-hornbeam forest (*Galium-carpinetum stachyetosum*) and allowed other tree species (especially maple), which are intolerant to flooding, to become dominant. Moreover, elm (*Ulmus minor*) largely disappeared from the tree canopy due to the Dutch Elm Disease since the 1960s. Nowadays, the dominant tree species of Leipzig's floodplain forest are *Quercus robur L.* (oak), *Acer pseudoplatanus L.* (maple) and *Fraxinus excelsior L.* (ash)[50,52], on which we focus in the present study. The floodplain soils originated from an accumulation of alluvial sediments, such as gravel, sand and loam, as result of several glacial periods[50]. These are nowadays covered by an alluvial clay layer with a thickness between 1-4 m,

rich in nutrients and with a high pH (around 6-7), whose deposition is closely linked to historic human settlements and deforestation[49,50]. The principal soil available to trees is thus a loamy Vega, with partly gleyed conditions, above gravel and sand filled with groundwater.

Drought year identification

The definition and identification of drought is central to the analysis of drought effects. Here, we define drought as period with water deficits compared to normal conditions, where 'normal' can be quantified as a percentile of the long-term mean of meteorological or hydrological variables[16,53]. Following suggestions by Schwarz *et al*[16] we selected drought years based on climatic and hydrological information alone without considering tree growth reductions to avoid a biased selection that could for example result in the exclusion of drought years without reduced growth. We used the Standardized Precipitation Evapotranspiration Index (SPEI)[39] and river discharge data to identify drought years. The SPEI is a commonly used drought index[7,16,29] based on the standardized monthly water balance of precipitation minus potential evapotranspiration. It can quantify drought severity according to a droughts intensity and duration and can be calculated at different time scales (e.g. 1-12 months)[39]. Here, we used three different SPEI lengths that represent the climatic water balance of the main vegetation period (SPEI for 3 months, Mai-July), the full vegetation period (SPEI for 6 months, April-September) and the full year (SPEI for 12 months, January-December) for each year and with a 40-year reference period (1979-2019; Supplementary Fig. 1). SPEIs were calculated with the SPEI package[54] in R from monthly precipitation (mm) and potential evapotranspiration (mm) data derived from the weather station located closest to the study sites (DWD, Station Leipzig/Halle, ID 2932; Supplementary Fig. 1).

We classified years with SPEI values ≤ -1 as drought years, years with SPEI values ≥ 1 as particularly wet and years with values between -1 and 1 as 'normal'[55]. To take into account the hydrological regime of the floodplain forest, which is in addition to local precipitation strongly influenced by its rivers, we compared the SPEI derived classification to river discharge calculated for the same periods as the SPEIs (Supplementary Fig. 2). We considered only years without particularly high discharge as drought years. Focusing on a 20-year period before the 2018-2019 consecutive drought, we selected 2005, 2009 and 2017 as reference years with normal climatic conditions, while single drought years – in contrast to the 2018-2019 consecutive drought – were 2003, 2006 and 2015 (Fig. 1; Supplementary Figs. 1-2). We did not consider a longer period to minimize the effect of past forest management and ground water fluctuation related influences on tree growth. Both, the drought in 2018 and the one in 2019 were the most severe droughts in the last 40 years (i.e. they had the lowest SPEI values), but 2018 had slightly lower SPEI values and was especially characterized by an extreme heat wave during the vegetation period.

Tree selection and increment core extraction

We selected trees for extracting wood increment cores from permanent forest research plots of the "Lebendige Luppe" (living Luppe river) project[56], which cover a gradient in topographic distances to the groundwater level (Supplementary Fig. 6). The project features three distinct strata of distance to groundwater: dry (> 2m), intermediate (1-2m) and wet (≤ 1m) plots, with 20 plots per stratum each 0.25ha in size. Plots were not flooded since 1973 due to flood control measures (dikes, river-straightening etc.), except for a relatively short period in winter 2011 and summer 2013, when the area of Leipzig experienced extreme flood events. We chose to sample trees on dry and wet plots to cover both ends of the gradient of hydrological site conditions within the

floodplain forest (Supplementary Fig. 6). Across these plots, we extracted tree increment cores from at least 40 tree individuals per species (20 trees per stratum) from each of the three dominant tree species oak, maple and ash, amounting to 120 sampled trees. From each tree, we extracted one increment core at a height of 80cm with a Ø 5mm increment corer (Suunto, Sweden) in January-February 2020. Trees with diameters at breast height (dbh) > 20cm were selected according to their dominance, past management history and health status. Competition for light is a central determinant of tree growth and $\delta^{13}C$ that might complicate the detection of drought effects[17]. We therefore sampled only dominant and co-dominant individuals, i.e. trees belonging to category 1-2 according to the classification of Kraft[57], that were no direct competitors and further excluded plots that showed signs of forest management in recent years. We further selected only healthy appearing trees, excluding those ash trees visually affected by 'ash dieback' (*Hymenoscyphus fraxineus*) and those maple trees visually affected by the 'sooty bark disease' (*Cryptostroma corticale*). Both fungal pathogens had caused widespread tree damages and diebacks in the Leipzig floodplain forest during the 2018-2019 consecutive drought and especially very few ash trees were completely unaffected[43]. We used the classification key of Lenz *et al.*[58] for ash dieback infestation and sampled only trees showing no to only little signs of infestation (level 0-2 of infestation levels 0-5) based on annual infestation records for four years prior sampling, while we sampled maple trees that showed no visual sign of sooty bark disease. Importantly, our sample is thus representative for the most vital individuals of the entire population. Since the number of trees fulfilling these strict criteria was too low within the plot area, we sampled also oak and maple trees in the direct vicinity of the plots.

403 **Tree growth analysis**

404 Tree cores were dried at 70 °C for at least 3 days and then clamped in wooden alignment strips.
405 For surface preparation, we used a core microtome (WSL, Switzerland)[59] to enhance visibility of
406 tree ring boundaries. Tree ring-width was measured with a LINTAB 6 measuring table and the
407 TSAPWin Professional 4.64 program © 2002-2009 Frank Rinn / RINNTECH with an accuracy of
408 1/1000 mm. The measured sequences were cross-dated against a species-specific master
409 chronology developed in former works for the same area as well as against each other using
410 COFECHA[60]. This allowed us to identify missing rings, which were more often found in maple
411 trees and in the consecutive drought years 2018-2019. Years without growth were included as zero
412 for the respective year. Sequences that could not be dated unequivocally were excluded from
413 further analysis. The final number of trees included for growth analysis was 114 trees instead of
414 the planned 120, including 40 oak, 32 maple and 42 ash trees from 11 wet and 15 dry plots.
415
416 Tree ring-width provides an integrated record of past growth conditions as influenced by
417 environmental factors including but not limited to climate and shows an inherent decrease in ring-
418 width with increasing tree size[14]. As we focus here on climatic influences on growth, we removed
419 age-related trends from the raw tree ring-width chronologies via a Negative Exponential curve[61],
420 which provided the best compromise between removing long-term age trends and preserving
421 decadal variability in growth using the package dplR[62,63]. We assessed the climatic sensitivity of
422 tree growth through computing bootstrapped Pearson's correlation functions between species-
423 specific chronologies and monthly climatic variables (Supplementary Fig. 5), using the package
424 treeclim[64].
425

We used tree growth resistance to the consecutive drought years 2018 and 2019 as well as to single drought years as indicator for tree growth responses to drought. Growth resistance for each individual tree was calculated following Lloret *et al*.[15] as:

$$Growth\ resistance = \frac{Dr_{growth}}{PreDr_{growth}} - 1 \quad (1)$$

where Dr_{growth} is a tree's growth in drought year(s) and $PreDr_{growth}$ is a tree's growth in the reference period characterized by normal climatic conditions. Growth resistance is thus standardized around zero with positive values meaning higher and negative values lower growth during drought year(s) compared to reference years. We calculated growth resistance for 2018, 2019 and for single drought years (using their mean growth resistance in all analysis). Recent decades experienced an unprecedented surge in temperatures and drought events[5,8], making the use of a continuous reference period of several years before drought events that is not influenced by drought itself difficult. We therefore used the mean growth in three years (2005, 2009, 2017) that were characterized by normal climatic conditions and not proceeded by a drought year (see above; Supplementary Fig. 1) to calculate $PreDr_{growth}$. We used several years to calculate $PreDr_{growth}$ and resistance in single drought years as this should reduce the influence of outliers caused by individual tree reactions to other factors than climate (e.g. changes in competitive interactions, waterlogging). However, as the choice of growth data and a reference period can strongly influence results on tree growth resistance to drought[16], we tested for the robustness of here reported relationships. We examined tree growth dynamics and growth resistance in detail based on raw and detrended ring-width and further compared resistance calculated with a 1-year pre-period (2017 was the only climatically normal year before the 2018-2019 consecutive drought;

449 Supplementary Fig. 1) to resistance calculated with the mean reference period detailed above.
450 Trends in growth resistance between years were consistent for all species (Fig. 2a-c;
451 Supplementary Figs. 3-4).
452
453 **Carbon isotope analysis**
454 The stable carbon isotope composition ($\delta^{13}C$) in wood of the same cores was measured after
455 completing tree ring-width measurements. The tree rings of the herein analysed consecutive
456 drought years 2018-2019, of single drought years (2003, 2006, 2015) and of reference years (2005,
457 2009, 2017) were separated and their wood tissue homogenized. Some trees, especially maple
458 ones, did not form tree rings during the 2018-2019 consecutive drought, likely due to intense
459 drought stress. As their $\delta^{13}C$ could thus not be analysed, we excluded these trees from our isotope
460 analysis (6 maple and 1 oak tree). The homogenized material of the tree rings in reference years
461 (2005, 2009 and 2017) and single drought years (2003, 2006 and 2015), was pooled by mixing
462 equal shares of the material from each of the three years. The isotope analysis was done at the
463 BGC stable isotope laboratory of the Max Planck Institute for Biogeochemistry in Jena, Germany.
464 The results were expressed as isotopic ratio $\delta^{13}C$, calculated with the equation of Farquhar *et al.*[19]
465 as follows:
466
467 $$\delta^{13}C = \left(\frac{\delta^{13}C\ (sample)}{\delta^{13}C(standard)} - 1\right) * 1000‰ \quad (2)$$
468
469 where $\delta^{13}C\ (sample)$ and $\delta^{13}C\ (standard)$ are the abundance ratios between ^{13}C and ^{12}C of the given
470 sample and Vienna PeeDee Belemnite international standard (VPDB). Isotope ratios were
471 expressed in δ-notation in per mil units (‰). We calculated the increase in $\delta^{13}C$ from reference to

drought years for each individual tree as indicator of a tree's physiological stress response to drought as:

$$\Delta\delta^{13}C = Dr_{\delta^{13}C} - PreDr_{\delta^{13}C} \quad (3)$$

where $Dr_{\delta^{13}C}$ is the isotope composition in drought year(s) and $PreDr_{\delta^{13}C}$ the isotope composition in the reference years (see e.g. ref[17]). Positive values of $\Delta\delta^{13}C$ thus indicate higher and negative values lower stress during drought year(s) compared to reference years. Drought and reference years used to calculate $\Delta\delta^{13}C$ were the same as in the growth resistance analysis.

Statistical analysis

We used linear mixed-effect models (LMMs) to understand the effects of consecutive drought years on tree growth resistance and $\Delta\delta^{13}C$ in comparison to single drought years. We were further interested in understanding how these effects were modulated by changes in a trees distance to groundwater. We fitted species-specific LMMs for growth resistance and $\Delta\delta^{13}C$ with the packages lme4[65] and lmerTest[66] and a significance level of $\alpha=0.05$. Drought events (single droughts, 2018, 2019), groundwater level (dry > 2m, wet ≤ 1m) and their interaction were modelled as fixed effects, while tree identities nested within plots were used as nested random effects to account for differences between plots and for repeated measurements on each individual tree. We selected the most parsimonious model structure via backward model selection, first adjusting the fixed and then the random effect structure, using the step function in lmerTest. The most parsimonious LMM structure consistently retained only a fixed effect of drought event and tree identity nested within plots as random effects, indicating that water table did not strongly influence observed

495 relationships. Only for the growth resistance LMM of oak we found a significant interaction
496 (P=0.0413) between drought event and groundwater level, which however disappeared when using
497 non-detrended growth data or a 1-year reference period. Therefore, to report only the most robust
498 relationships, we present all final LMMs with drought event as the only fixed effect. Final LMMs
499 (Supplementary Table 1) were fit using restricted maximum likelihood estimation (REML) and
500 marginal means and confidence intervals (95%) were predicted with the ggeffects package[67]. We
501 used post-hoc pairwise comparisons with adjusted p-values for multiple comparisons (Tukey's
502 Honest Significant Difference) to compare differences between drought events using the emmeans
503 package[68] (Supplementary Table 2). Model assumptions (normality, independence and
504 homogeneity of variance) where visually checked through examining model residuals and through
505 quantile-quantile plots. All analyses were conducted in R version 4.0.3[69].
506

507 **Acknowledgements**

508 We thank our colleagues of the ‚Lebendige Luppe' (living Luppe river) project for establishing
509 the plot network that allowed us to draw representative conclusions and Andreas Sickert
510 (Stadtforst) und Andreas Padberg (Sachsenforst) for the possibility to extract tree increment cores.
511 The Lebendige Luppe project is funded by the German Federal Agency for Nature Conservation
512 (BfN) in cooperation with the German Federal Ministry for the Environment (BMU). We further
513 acknowledge the help of the BGC stable isotope laboratory of the Max Planck Institute for
514 Biogeochemistry in Jena, Germany. F.S. was supported by the International Research Training
515 Group TreeDì funded by the Deutsche Forschungsgemeinschaft (DFG, German Research
516 Foundation) – 319936945/GRK2324.
517

518 **Author contributions**

519 C.W., F.S., R.A.E., A.K., R.R., C.S.-D. and G.S. conceived the idea and developed the concept of
520 the study. S.P., L.S., A.K., F.S., R.A.E. and C.S.-D. collected data. F.S., S.P, L.S. and G.S.
521 analyzed data. F.S., C.S.-D. and G.S. created figures. F.S. wrote the manuscript with contributions
522 from S.P. and L.S. All authors discussed the results and contributed substantially to revisions.

523

524 # References

525 1. IPCC. *Climate change 2014. Impacts, Adaptation, and Vulnerability. Part A: Global and*
526 *Sectoral Aspects. Contribution of Working Group II to the Fifth Assessment Report of the*
527 *Intergovernmental Panel on Climate Change* (Cambridge University Press, New York, NY,
528 2014).

529 2. Allen, C. D. *et al.* A global overview of drought and heat-induced tree mortality reveals
530 emerging climate change risks for forests. *For. Ecol. Manage.* **259,** 660–684;
531 10.1016/j.foreco.2009.09.001 (2010).

532 3. Anderegg, W. R. L. *et al.* Climate-driven risks to the climate mitigation potential of forests.
533 *Science* **368**; 10.1126/science.aaz7005 (2020).

534 4. Griscom, B. W. *et al.* Natural climate solutions. *PNAS* **114,** 11645–11650;
535 10.1073/pnas.1710465114 (2017).

536 5. Buras, A., Rammig, A. & Zang, C. S. Quantifying impacts of the 2018 drought on European
537 ecosystems in comparison to 2003. *Biogeosciences* **17,** 1655–1672; 10.5194/bg-17-1655-
538 2020 (2020).

6. Allen, C. D., Breshears, D. D. & McDowell, N. G. On underestimation of global vulnerability to tree mortality and forest die-off from hotter drought in the Anthropocene. *Ecosphere* **6**; 10.1890/ES15-00203.1 (2015).

7. Hari, V., Rakovec, O., Markonis, Y., Hanel, M. & Kumar, R. Increased future occurrences of the exceptional 2018-2019 Central European drought under global warming. *Scientific Reports* **10,** 12207; 10.1038/s41598-020-68872-9 (2020).

8. Schuldt, B. *et al.* A first assessment of the impact of the extreme 2018 summer drought on Central European forests. *Basic Appl. Ecol.* **45,** 86–103; 10.1016/j.baae.2020.04.003 (2020).

9. Anderegg, W. R. L. *et al.* Pervasive drought legacies in forest ecosystems and their implications for carbon cycle models. *Science* **349,** 528–532 (2015).

10. Szejner, P., Belmecheri, S., Ehleringer, J. R. & Monson, R. K. Recent increases in drought frequency cause observed multi-year drought legacies in the tree rings of semi-arid forests. *Oecologia* **192,** 241–259; 10.1007/s00442-019-04550-6 (2020).

11. Kannenberg, S. A. *et al.* Linking drought legacy effects across scales: From leaves to tree rings to ecosystems. *Global Change Biol.* **25,** 2978–2992; 10.1111/gcb.14710 (2019).

12. Gazol, A. *et al.* Tree Species Are Differently Impacted by Cumulative Drought Stress and Present Higher Growth Synchrony in Dry Places. *Front. For. Glob. Change* **3**; 10.3389/ffgc.2020.573346 (2020).

13. Anderegg, W. R. L. *et al.* Drought's legacy: multiyear hydraulic deterioration underlies widespread aspen forest die-off and portends increased future risk. *Global Change Biol.* **19,** 1188–1196; 10.1111/gcb.12100 (2013).

14. Schweingruber, F. H. *Tree rings and environment: dendroecology* (Paul Haupt AG Bern, Berne, Switzerland, 1996).

15. Lloret, F., Keeling, E. G. & Sala, A. Components of tree resilience. Effects of successive low-growth episodes in old ponderosa pine forests. *Oikos* **120,** 1909–1920; 10.1111/j.1600-0706.2011.19372.x (2011).

16. Schwarz, J. *et al.* Quantifying Growth Responses of Trees to Drought—a Critique of Commonly Used Resilience Indices and Recommendations for Future Studies. *Curr. Forestry Rep.* **6,** 185–200; 10.1007/s40725-020-00119-2 (2020).

17. Grossiord, C. *et al.* Tree diversity does not always improve resistance of forest ecosystems to drought. *PNAS* **111,** 14812–14815; 10.1073/pnas.1411970111 (2014).

18. Jucker, T. *et al.* Detecting the fingerprint of drought across Europe's forests: do carbon isotope ratios and stem growth rates tell similar stories? *For. Ecosyst.* **4,** 706; 10.1186/s40663-017-0111-1 (2017).

19. Farquhar, G. D., Ehleringer, J. R. & Hubick, K. T. Carbon Isotope Discrimination and Photosynthesis. *Annu. Rev. Plant. Physiol. Plant. Mol. Biol.* **40,** 503–537; 10.1146/annurev.pp.40.060189.002443 (1989).

20. Choat, B. *et al.* Global convergence in the vulnerability of forests to drought. *Nature* **491,** 752–755; 10.1038/nature11688 (2012).

21. McDowell, N. *et al.* Mechanisms of plant survival and mortality during drought: why do some plants survive while others succumb to drought? *New Phytol.* **178,** 719–739; 10.1111/j.1469-8137.2008.02436.x (2008).

581 22. Martínez-Vilalta, J. & Garcia-Forner, N. Water potential regulation, stomatal behaviour and
582 hydraulic transport under drought: deconstructing the iso/anisohydric concept. *Plant Cell*
583 *Environ.* **40,** 962–976; 10.1111/pce.12846 (2017).

584 23. Mikac, S. *et al.* Drought-induced shift in tree response to climate in floodplain forests of
585 Southeastern Europe. *Scientific Reports* **8,** 16495; 10.1038/s41598-018-34875-w (2018).

586 24. Sánchez-Pérez, J. M., Lucot, E., Bariac, T. & Trémolières, M. Water uptake by trees in a
587 riparian hardwood forest (Rhine floodplain, France). *Hydrol. Processes* **22,** 366–375;
588 10.1002/hyp.6604 (2008).

589 25. Kutschera, L. & Lichtenegger, E. *Wurzelatlas mitteleuropäischer Waldbäume und Sträucher.*
590 6th ed. (Stocker, Graz, 2013).

591 26. Nardini, A. *et al.* Rooting depth, water relations and non-structural carbohydrate dynamics in
592 three woody angiosperms differentially affected by an extreme summer drought. *Plant, cell*
593 *& environment* **39,** 618–627; 10.1111/pce.12646 (2016).

594 27. Ward, J. V., Tockner, K. & Schiemer, F. Biodiversity of floodplain river ecosystems:
595 ecotones and connectivity1. *Regul. Rivers: Res. Mgmt.* **15,** 125–139; 10.1002/(SICI)1099-
596 1646(199901/06)15:1/3<125::AID-RRR523>3.0.CO;2-E (1999).

597 28. Leuschner, C. & Ellenberg, H. *Vegetation ecology of Central Europe. Vegetation Ecology of*
598 *Central Europe, Volume I* (Springer, Cham, Switzerland, 2017).

599 29. Skiadaresis, G., Schwarz, J. A. & Bauhus, J. Groundwater Extraction in Floodplain Forests
600 Reduces Radial Growth and Increases Summer Drought Sensitivity of Pedunculate Oak Trees
601 (Quercus robur L.). *Front. For. Global Change* **2,** 267; 10.3389/ffgc.2019.00005 (2019).

30. Tockner, K. & Stanford, J. A. Riverine flood plains: present state and future trends. *Environ. Conserv.* **29,** 308–330; 10.1017/S037689290200022X (2002).

31. Kowalska, N. *et al.* Analysis of floodplain forest sensitivity to drought. *Philosophical transactions of the Royal Society of London. Series B, Biological sciences* **375,** 20190518; 10.1098/rstb.2019.0518 (2020).

32. Heklau, H., Jetschke, G., Bruelheide, H., Seidler, G. & Haider, S. Species-specific responses of wood growth to flooding and climate in floodplain forests in Central Germany. *iForest* **12,** 226–236; 10.3832/ifor2845-012 (2019).

33. Brunotte, E., Dister, E., Günther-Diringer, D., Koenzen, U. & Mehl, D. Flussauen in Deutschland . Erfassung und Bewertung des Auenzustandes. *Naturschutz und Biologische Vielfalt* **87**.

34. BMU & BfN - Bundesministerium für Umweltschutz und Bundesamt für Naturschutz. Auenzustandsbericht. Flussauen in Deutschland, 2009.

35. Cocozza, C. *et al.* Isotopic and Water Relation Responses to Ozone and Water Stress in Seedlings of Three Oak Species with Different Adaptation Strategies. *Forests* **11,** 864; 10.3390/f11080864 (2020).

36. Thomsen, S., Reisdorff, C., Gröngröft, A., Jensen, K. & Eschenbach, A. “Responsiveness of mature oak trees (Quercus robur L.) to soil water dynamics and meteorological constraints in urban environments”. *Urban Ecosyst* **23,** 173–186; 10.1007/s11252-019-00908-z (2020).

37. Leuschner, C., Wedde, P. & Lübbe, T. The relation between pressure–volume curve traits and stomatal regulation of water potential in five temperate broadleaf tree species. *Ann. For. Sci.* **76**; 10.1007/s13595-019-0838-7 (2019).

624 38. Lemoine, D., Peltier, J.-P. & Marigo, G. Comparative studies of the water relations and the
625 hydraulic characteristics in Fraxinus excelsior, Acer pseudoplatanus and A. opalus trees
626 under soil water contrasted conditions. *Ann. For. Sci.* **58,** 723–731; 10.1051/forest:2001159
627 (2001).

628 39. Vicente-Serrano, S. M., Beguería, S. & López-Moreno, J. I. A Multiscalar Drought Index
629 Sensitive to Global Warming. The Standardized Precipitation Evapotranspiration Index. *J.*
630 *Clim.* **23,** 1696–1718; 10.1175/2009JCLI2909.1 (2010).

631 40. Deutscher Wetterdienst. Klimastatusbericht Deutschland Jahr 2019. DWD, Geschäftsbereich
632 Klima und Umwelt, 2020.

633 41. Singer, M. B. *et al.* Floodplain ecohydrology: Climatic, anthropogenic, and local physical
634 controls on partitioning of water sources to riparian trees. *Water resources research* **50,**
635 4490–4513; 10.1002/2014WR015581 (2014).

636 42. Hartmann, H. & Trumbore, S. Understanding the roles of nonstructural carbohydrates in
637 forest trees - from what we can measure to what we want to know. *New Phytol.* **211,** 386–
638 403; 10.1111/nph.13955 (2016).

639 43. Wirth, C. *et al.* Naturschutz und Klimawandel im Leipziger Auwald. Ein
640 Biodiversitätshotspot an der Belastungsgrenze. *Biol. unserer Zeit* **51,** 55–65 (2021).

641 44. Richardson, A. D. *et al.* Seasonal dynamics and age of stemwood nonstructural carbohydrates
642 in temperate forest trees. *The New phytologist* **197,** 850–861; 10.1111/nph.12042 (2013).

643 45. Scharnweber, T., Manthey, M. & Wilmking, M. Differential radial growth patterns between
644 beech (Fagus sylvatica L.) and oak (Quercus robur L.) on periodically waterlogged soils.
645 *Tree Physiol.* **33,** 425–437; 10.1093/treephys/tpt020 (2013).

646 46. Weil, R. R. & Brady, N. C. *Nature and properties of soils.* 15th ed. (Pearson, 2017).

647 47. Montgomery, R. A., Reich, P. B. & Palik, B. J. Untangling positive and negative biotic
648 interactions: views from above and below ground in a forest ecosystem. *Ecology* **91,** 3641–
649 3655; 10.1890/09-1663.1 (2010).

650 48. Schnabel, F. *et al.* Drivers of productivity and its temporal stability in a tropical tree diversity
651 experiment. *Global Change Biol.* **25,** 4257-4272; 10.1111/gcb.14792 (2019).

652 49. Gutte, P. Das Querco-Ulmetum minoris ISSLER 1942, der Stieleichen-Ulmen-Hartholzwald,
653 in der Elster-Luppe-Aue bei Leipzig. *Mauritiana* **22,** 213–242 (2011).

654 50. Haase, D. & Gläser, J. Determinants of floodplain forest development illustrated by the
655 example of the floodplain forest in the District of Leipzig. *For. Ecol. Manage.* **258,** 887–894;
656 10.1016/j.foreco.2009.03.025 (2009).

657 51. Härdtle, W. *et al.* Pflanzengesellschaft des Jahres 2021: Hartholz-Auenwald (Ficario-
658 Ulmetum). *Tuexenia* **40,** 373–399.

659 52. Richter, R., Reu, B., Wirth, C., Doktor, D. & Vohland, M. The use of airborne hyperspectral
660 data for tree species classification in a species-rich Central European forest area. *Int. J. Appl.*
661 *Earth Obs. Geoinf.* **52,** 464–474; 10.1016/j.jag.2016.07.018 (2016).

662 53. van Loon, A. F. *et al.* Drought in a human-modified world: reframing drought definitions,
663 understanding, and analysis approaches. *Hydrol. Earth Syst. Sci.* **20,** 3631–3650;
664 10.5194/hess-20-3631-2016 (2016).

665 54. Beguería, S. & Vicente-Serrano, S. M. *SPEI: Calculation of the Standardised Precipitation-*
666 *Evapotranspiration Index.* (2017).

667 55. McKee, T. B., Doesken, N. J. & Kleist, J. The relationship of drought frequency and duration
668 to time scales. In *Proceedings of the 8th Conference on Applied Climatology* (1993), Vol. 17,
669 pp. 179–183.

670 56. Scholz, M. *et al.* Das Projekt Lebendige Luppe – ein Beitrag zur Renaturierung der Leipziger
671 Nord-West-Aue. *Auenmagazin* **14,** 14–21 (2018).

672 57. Kraft, G. *Beiträge zur Lehre von den Durchforstungen, Schlagstellungen und*
673 *Lichtungshieben* (Klindworth's Verlag, Hannover, Germany, 1884).

674 58. Lenz, H., Straßer, L., Baumann, M. & Baie, U. Boniturschlüssel zur Einstufung der Vitalität
675 von Alteschen. *AFZ-DerWald* **3,** 18–19 (2012).

676 59. Gärtner, H. & Nievergelt, D. The core-microtome: A new tool for surface preparation on
677 cores and time series analysis of varying cell parameters. *Dendrochronologia* **28,** 85–92;
678 10.1016/j.dendro.2009.09.002 (2010).

679 60. Grissino-Mayer, H. D. Evaluating Crossdating Accuracy: A Manual and Tutorial for the
680 Computer Program COFECHA. *Tree-Ring Research* (2001).

681 61. Fritts, H. *Tree Rings and Climate* (Academic Press, London, UK, 1976).

682 62. Bunn, A. G. A dendrochronology program library in R (dplR). *Dendrochronologia* **26,** 115–
683 124; 10.1016/j.dendro.2008.01.002 (2008).

684 63. Bunn, A. G. *et al. dplR: Dendrochronology Program Library in R*. Available at
685 https://CRAN.R-project.org/package=dplR (2020).

686 64. Zang, C. & Biondi, F. treeclim: an R package for the numerical calibration of proxy-climate
687 relationships. *Ecography* **38,** 431–436; 10.1111/ecog.01335 (2015).

65. Bates, D., Mächler, M., Bolker, B. & Walker, S. Fitting Linear Mixed-Effects Models Using lme4. *J. Stat. Softw.* **67**; 10.18637/jss.v067.i01 (2015).

66. Kuznetsova, A., Brockhoff, P. B. & Christensen, R. H. B. lmerTest Package: Tests in Linear Mixed Effects Models. *J. Stat. Softw.* **82**; 10.18637/jss.v082.i13 (2017).

67. Lüdecke, D. ggeffects: Tidy Data Frames of Marginal Effects from Regression Models. *J. Open Source Softw.* **3,** 772; 10.21105/joss.00772 (2018).

68. Lenth, R. *emmeans: Estimated Marginal Means, aka Least-Squares Means.* (2020).

69. R Core Team. *A language and environment for statistical computing* (R Foundation for Statistical Computing, Vienna, Austria, 2020).